

Supplementary Information for *Contribution to the coordination chemistry of transition metal nitroprussides. A cryo-XPS study*, by A. Cano, L. Lartundo-Rojas, A. Shchukarev and E. Reguera

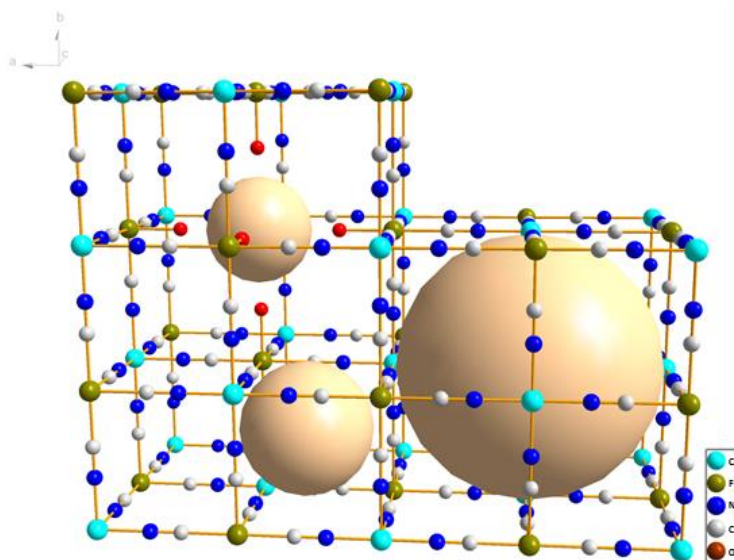


Figure S1. Atomic packing for the cubic phase of $T[\text{Fe}(\text{CN})_5\text{NO}]\cdot x\text{H}_2\text{O}$, $T = \text{Fe}, \text{Co}, \text{Ni}$. This subseries of cubic metal nitroprussides has a porous framework formed by three types of cavities. The large sphere corresponds to the largest cavity due to vacancies for the building block, $[\text{Fe}(\text{CN})_5\text{NO}]$. For Fe and Co, the orthorhombic structure ($Pnma$) is also possible (see Figure S2).

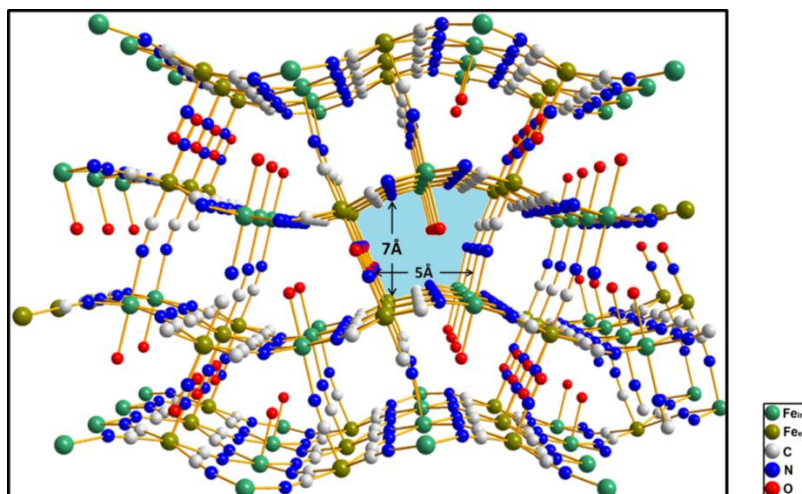


Figure S2. Atomic packing for orthorhombic metal nitroprussides, $T[\text{Fe}(\text{CN})_5\text{NO}]$ with $T = \text{Mn}, \text{Fe}, \text{Co}, \text{Zn}, \text{Cd}$. For Fe and Co the cubic ($Fm\bar{3}m$) phase is also possible (Figure S1).

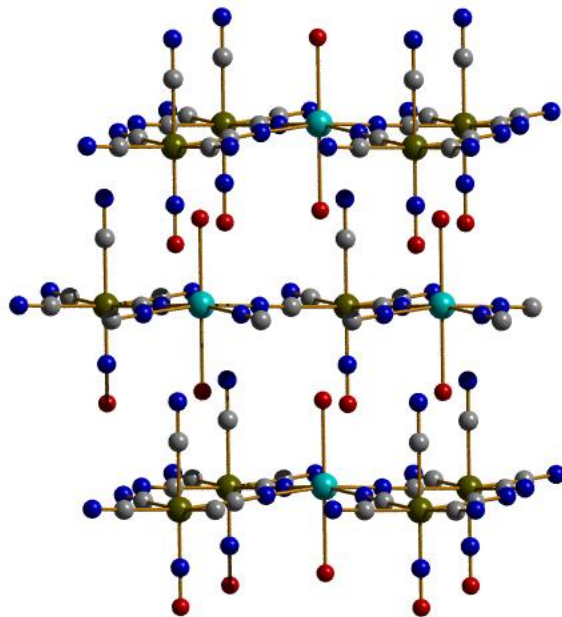


Figure S3: Atomic packing within the unit cell for 2D copper nitroprusside, $\text{Cu}(\text{H}_2\text{O})_2[\text{Fe}(\text{CN})_5\text{NO}]$.

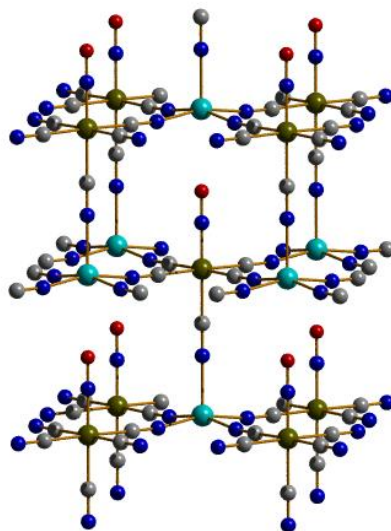


Figure S4: Atomic packing within the unit cell anhydrous copper nitroprusside, $\text{Cu}[\text{Fe}(\text{CN})_5\text{NO}]$. This material has a 3D framework where the copper atom appears with a square-base pyramidal coordination.

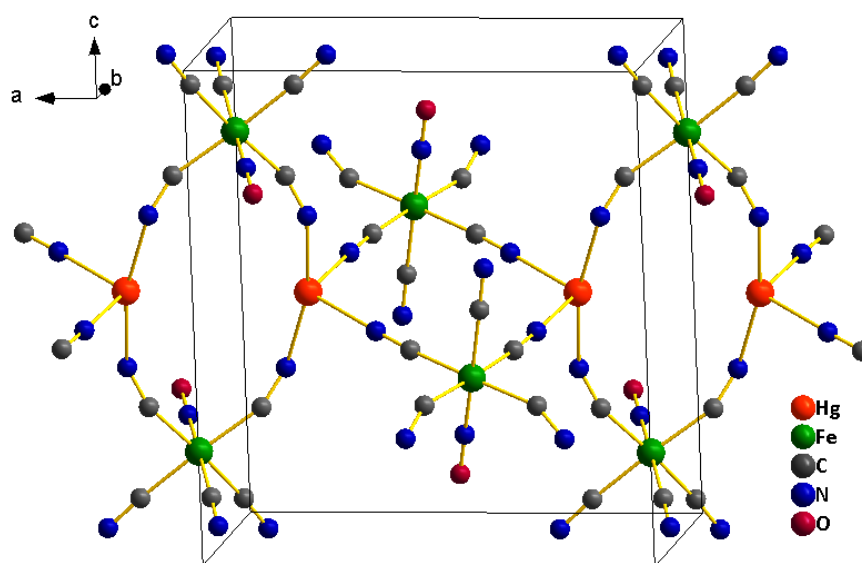


Figure S5: Atomic packing within the unit cell and porous framework for $\text{Hg}[\text{Fe}(\text{CN})_5\text{NO}]$.

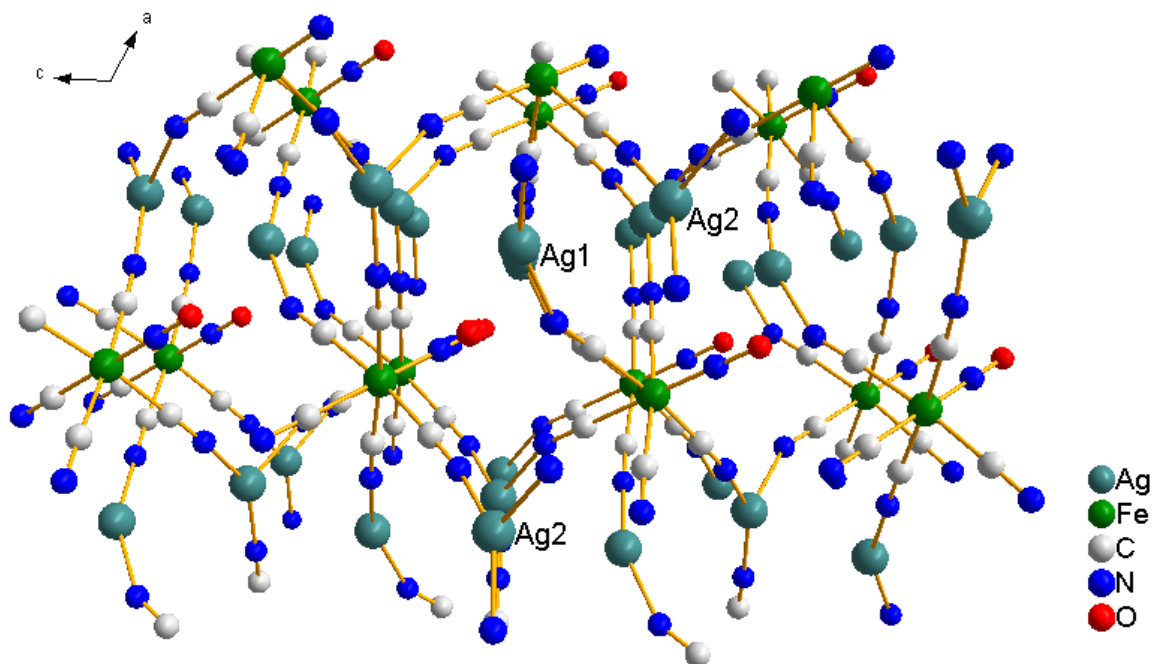


Figure S6: Framework of silver nitroprusside and coordination environments for the involved metals (Fe and Ag). In the structure, there are two types silver atoms (Ag1 and Ag2) at a distance of $3.165(3) \text{ \AA}$. The NO group remains unlinked at its O end.

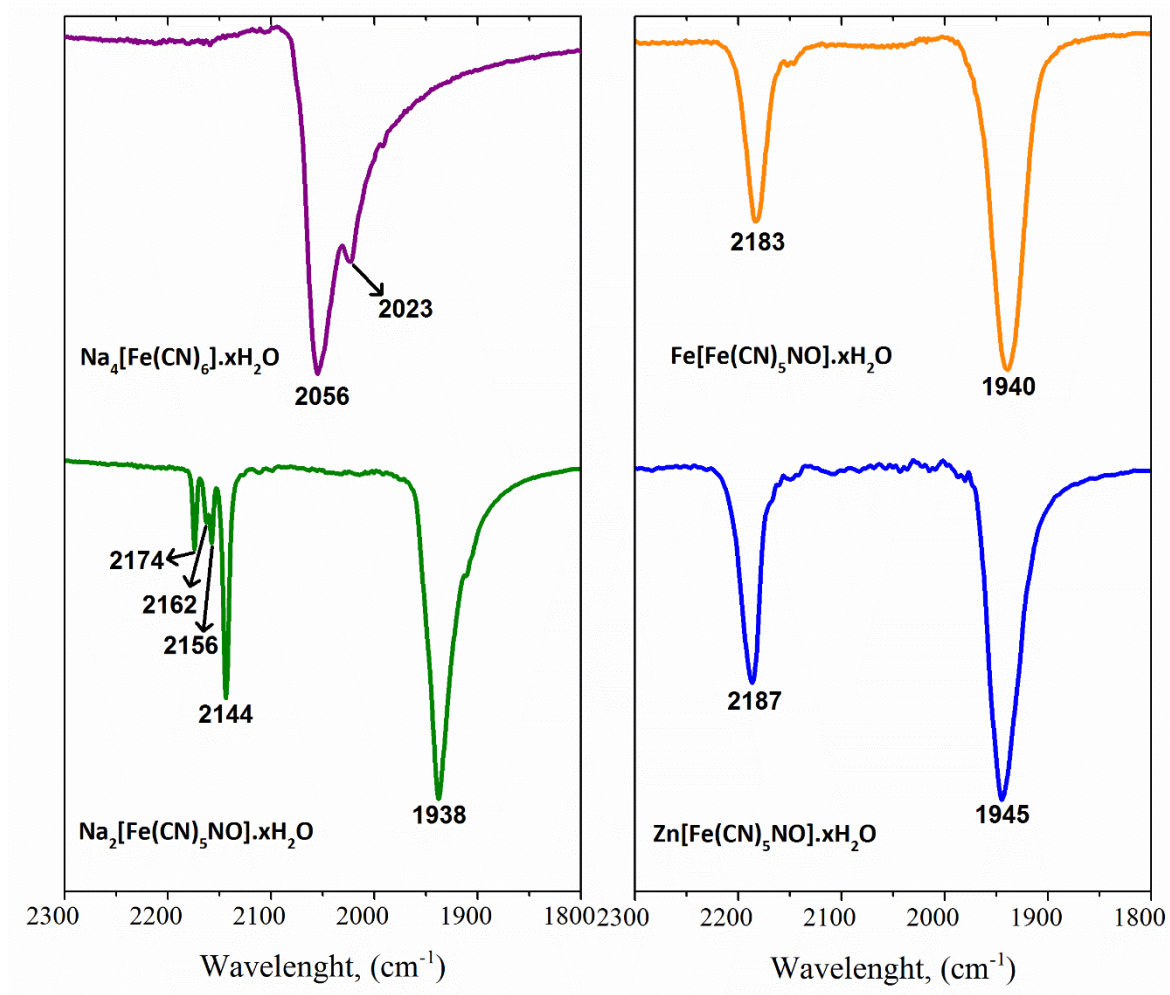


Figure S7: IR spectra for: (Left) sodium ferrocyanide and sodium nitroprusside; (Right) ferrous nitroprusside (cubic phase) and zinc(2+) nitroprusside (orthorhombic phase).

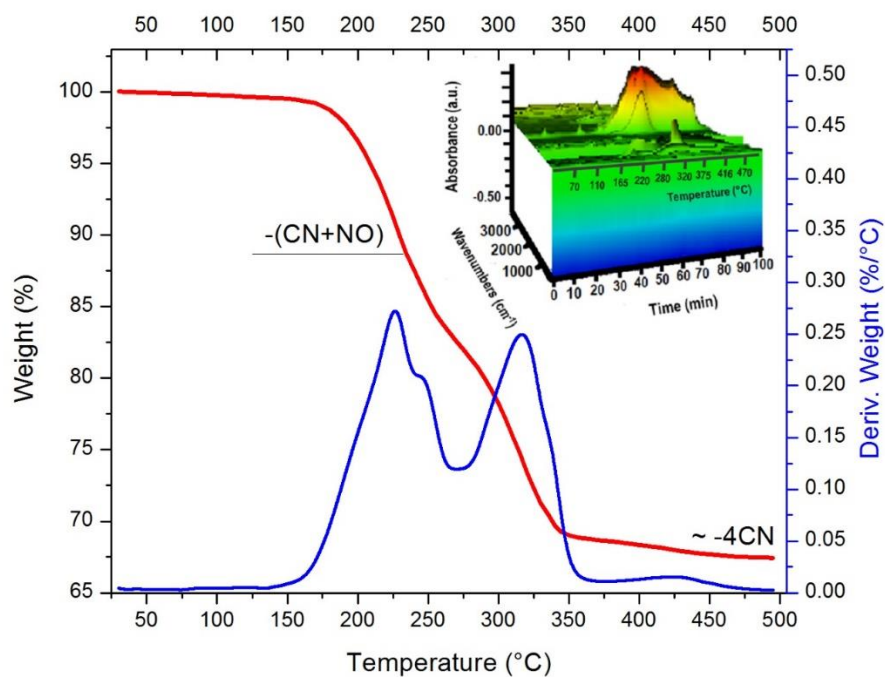


Figure S8: TG curve recorded under a nitrogen atmosphere for silver nitroprusside. Inset: Normalized IR spectra of the evolved gases on the sample heating.

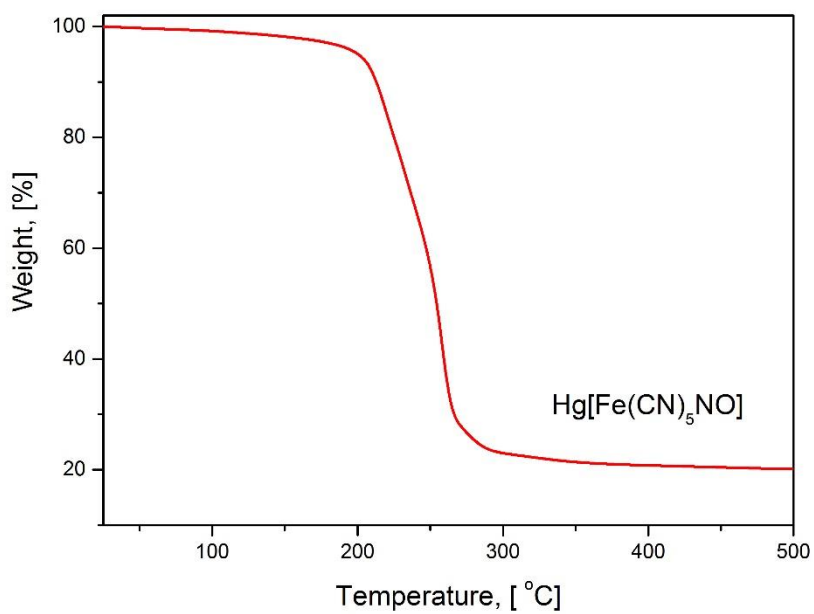


Figure S9: TG curve recorded under a nitrogen atmosphere for mercury (2+) nitroprusside

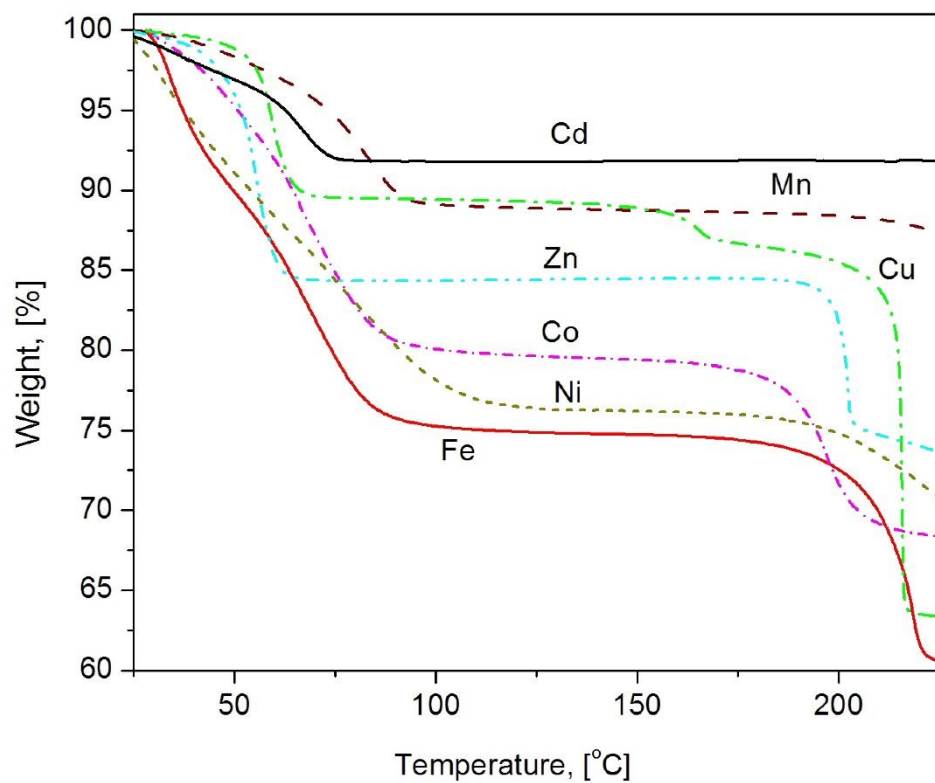


Figure S10: TG curve recorded under a nitrogen atmosphere for divalent transition metal nitroprussides. The weight lost observed below 100 °C corresponds to the evolution of water molecules. Then, the resulting anhydrous solids show certain structural stability.

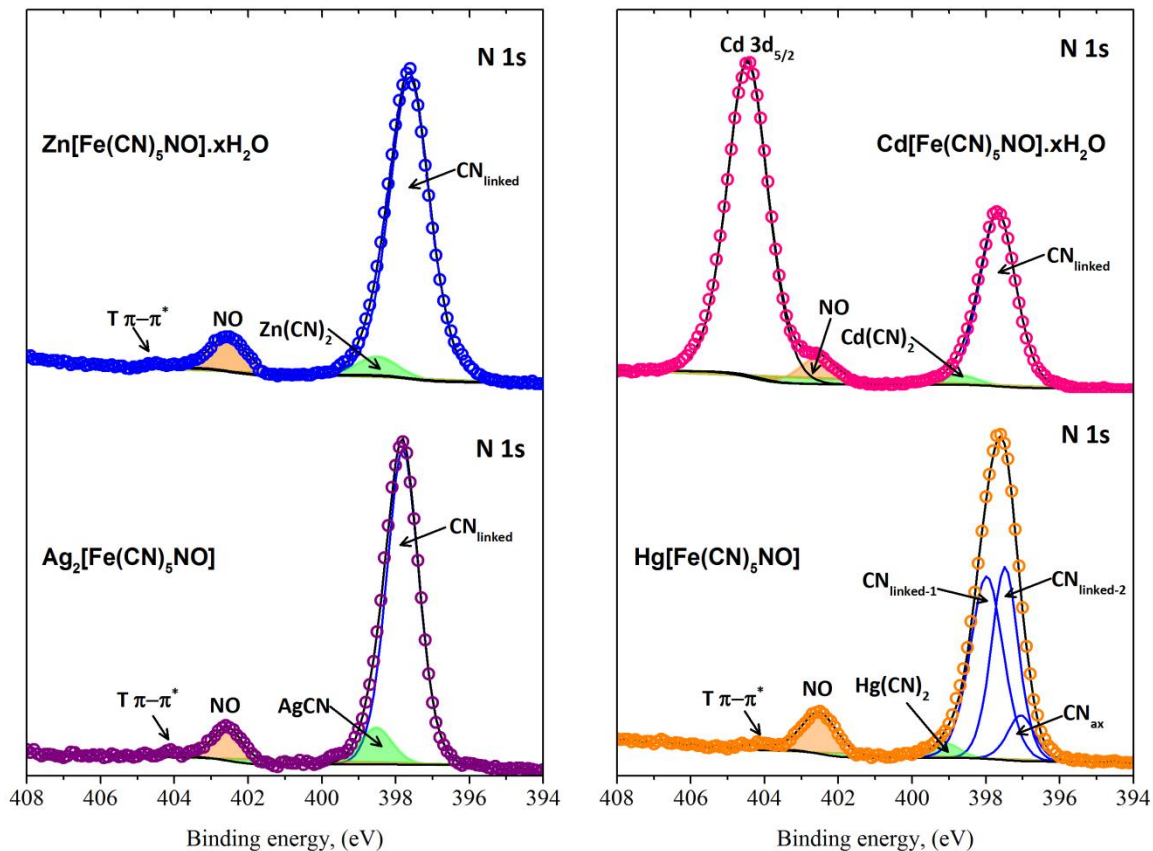


Figure S11. N 1s spectral region for the subseries $\text{Ag}_2[\text{Fe}(\text{CN})_5\text{NO}]$ and $\text{T}[\text{Fe}(\text{CN})_5\text{NO}]$ with $\text{T} = \text{Zn}, \text{Cd}, \text{Hg}$. Indicated are the N 1s peak (shaded peak in green) for the metal cyanide minor fraction resulting from the sample degradation under its interaction with the X-ray beam. For Hg at least three N 1s peaks were resolved, in accordance with the crystal structure of this compound [21]. The assignment of the N 1s peak corresponding to the simple metal cyanides, is supported by the study of these compounds as pure phases (see below).

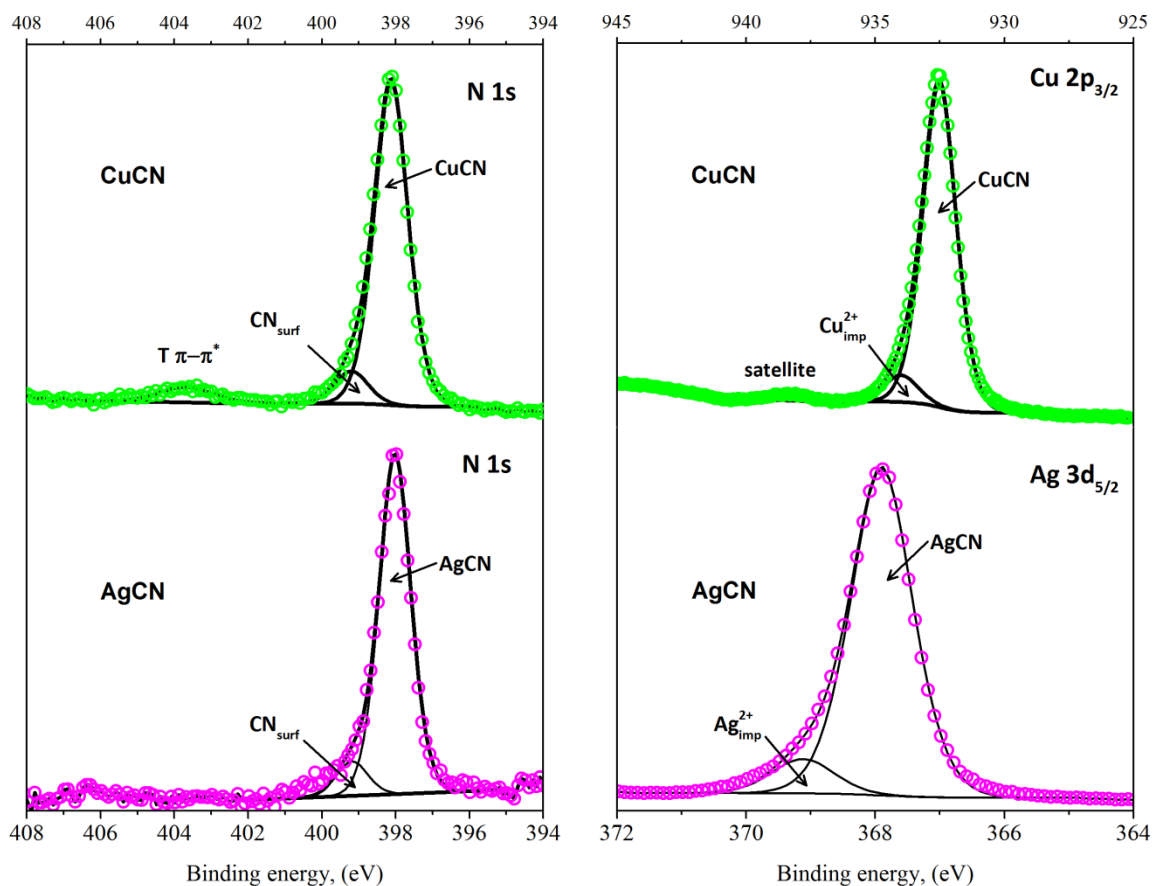


Figure S12: N 1s, Cu 2p and Ag 3d_{5/2} spectral regions for CuCN and AgCN. For both compounds a minor fraction of oxidized species for the metal were identified.

Table S1: N 1s and Metal binding energy (in eV) from the XPS spectra of AgCN, CuCN and Zn(CN)₂

Metal cyanide	N1s _{CN}	N1s _{CN_surf}	T π-π*	Metal	M _{imp}	satellite
AgCN	398.1	399.2	403.7	932.5	934	-
CuCN	398	399.2	-	367.9	369.1	938.3
Zn(CN) ₂	398.3	399.7	-	1021.1	-	-

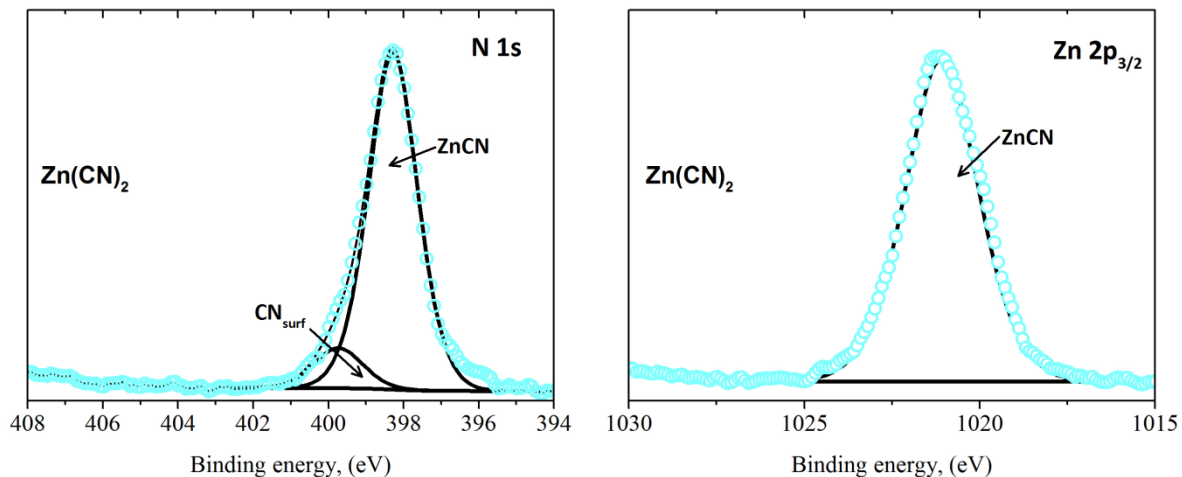


Figure S13: N 1s and Zn 2p_{3/2} spectral regions for Zn(CN)₂. The Zn 2p_{3/2} shown a significant broadening, which was ascribed to the presence of different coordination environment for the Zn atom in the crystal structure of this coordination polymer, ...NC-Zn-CN..., ...NC-Zn-NC..., ...CN-Zn-NC...

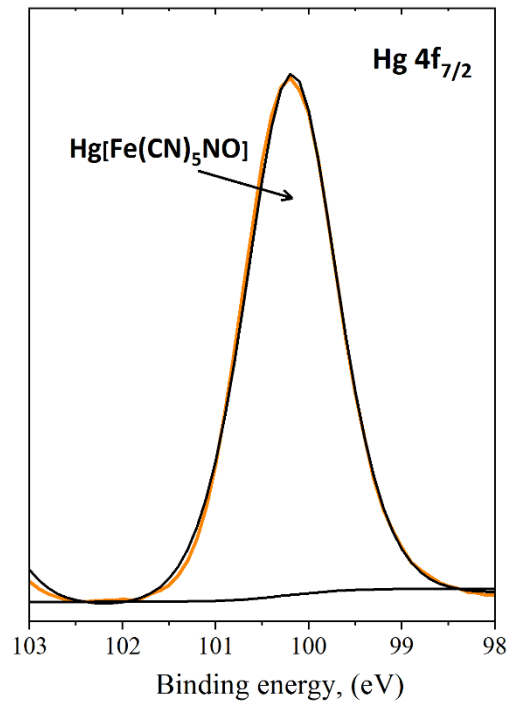


Figure S14. Spectral profile for Hg 4f_{7/2} core level in Hg(2+) nitroprusside. The Auger lines for Hg(2+) must be observed in the 1380 -1412 eV spectral region. The used X-ray source was AlK α , with a work energy window limited up to 1400 eV, and in sequence, without possibility for the Hg Auger lines recording.

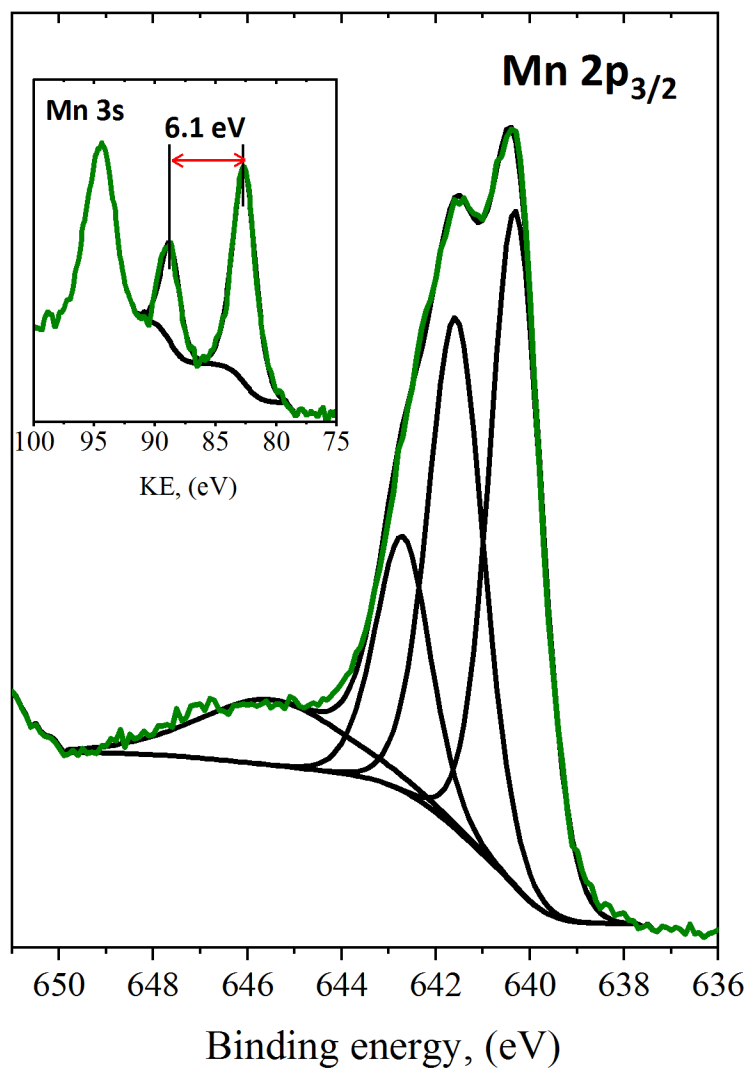


Figure S15. Spectral region for Mn 2p_{3/2} core level in Mn(2+) nitroprusside. The observed XPS spectrum corresponds to Mn(2+). This was confirmed by the spectrum corresponding to Mn 3s core level peaks (Inset)

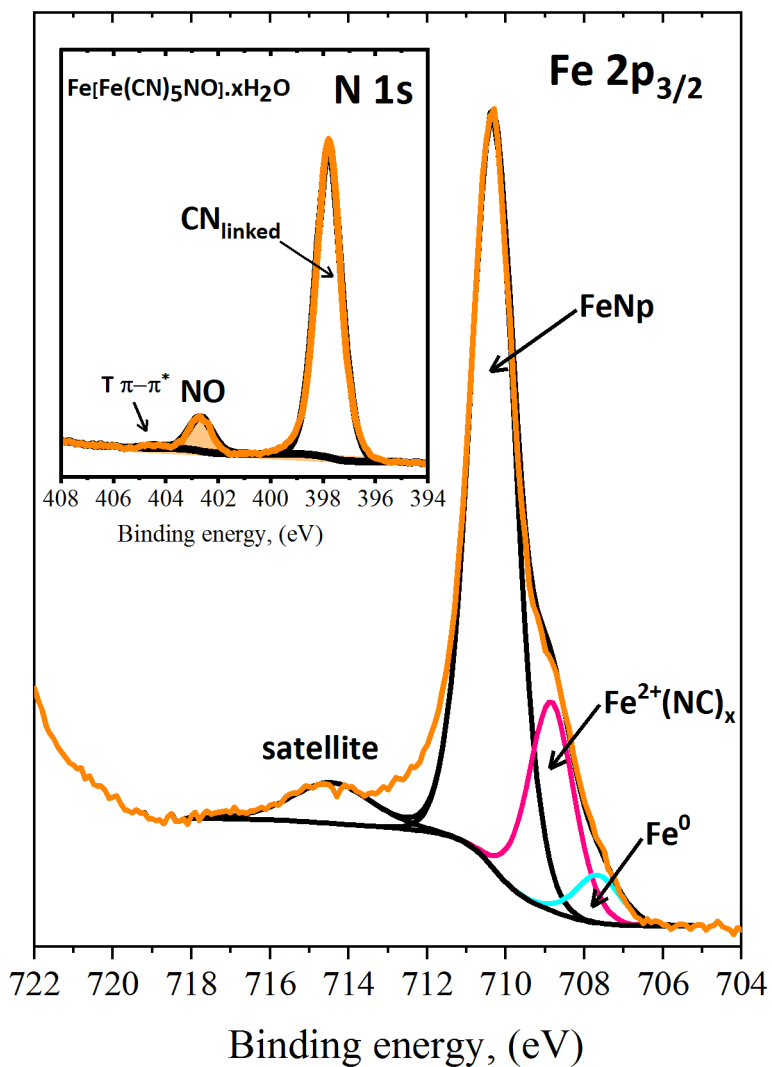


Figure S16. Spectral region for Fe 2p_{3/2} core level spectrum in Fe(2+) nitroprusside. The observed XPS spectrum corresponds to a superposition of peaks from low spin Fe(II), high spin Fe(2+) and metallic iron (Fe⁰). Inset: N 1s spectral region

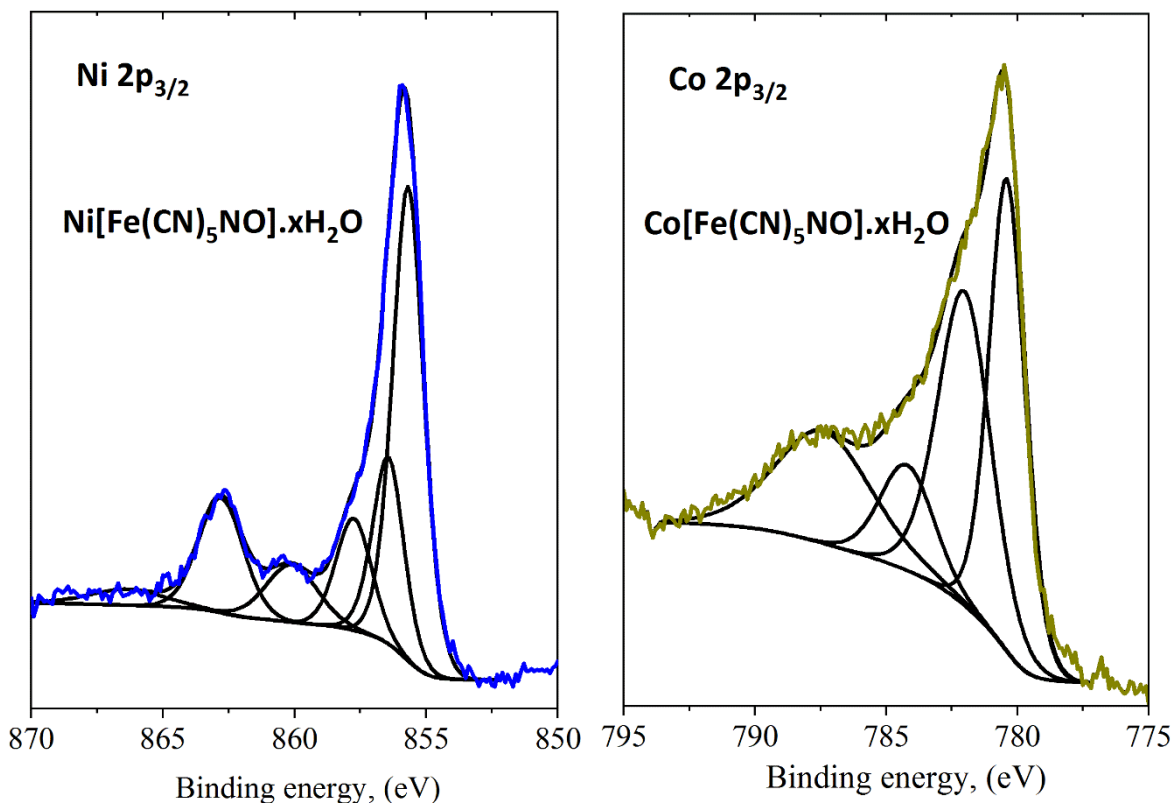


Figure S17. Spectral region for Co 2p_{3/2} and Ni 2p_{3/2} core level spectra in Co(2+) and Ni(2+) nitroprussides. These spectra have a complex structure related to the appearance of multiple splitting for these two cations. The satellite peaks at high energy provide conclusive clue of their nature as presence of divalent Co(2+) and Ni(2+) cations. The peak located at 860 eV for the sample of Ni nitroprusside remains unassigned.

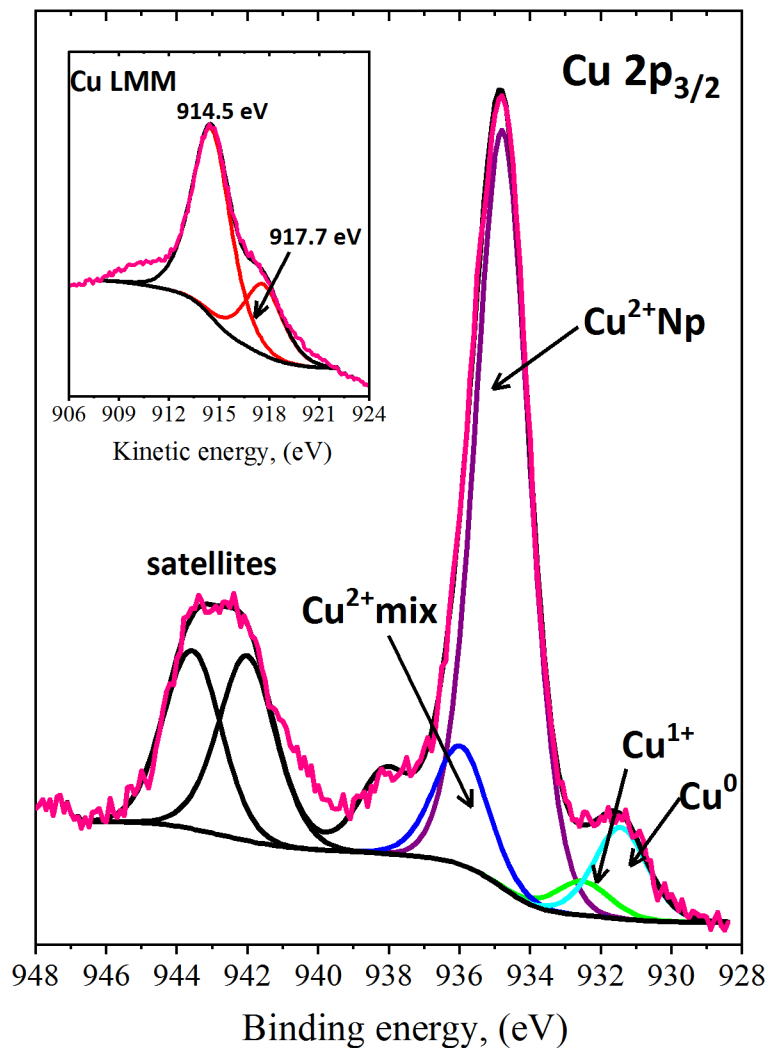


Figure S18. Spectral region for Cu 2p_{3/2} core level spectrum in Cu (2+) nitroprusside. In addition to the copper (2+) atom in copper nitroprusside, reduced species of copper (+) as copper (+) cyanide, CuCN, and Cu⁰ were identified.

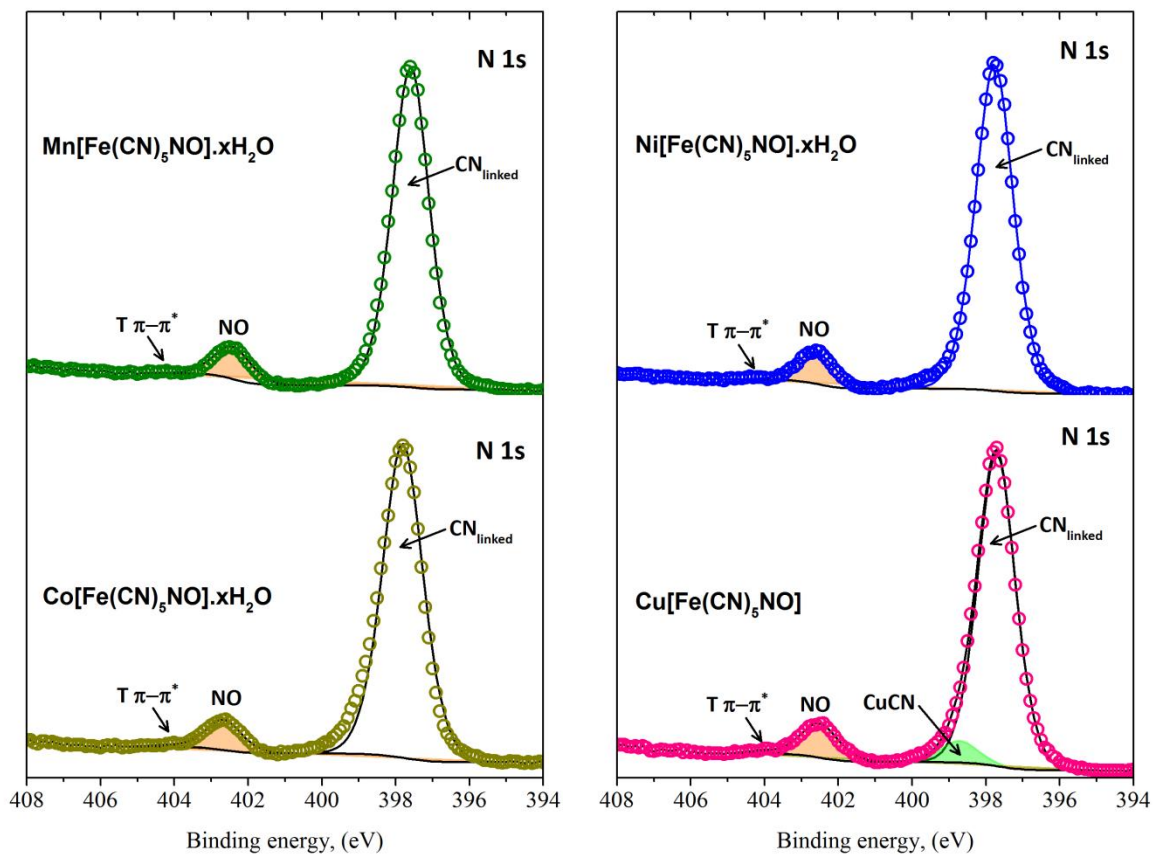


Figure S19. N 1s spectral region for the subseries $T[\text{Fe}(\text{CN})_5\text{NO}]$ with $T = \text{Mn}, \text{Co}, \text{Ni}, \text{Cu}$. For Cu, CuCN is formed during the sample degradation under its interaction with the X-ray beam (see Figure S11).

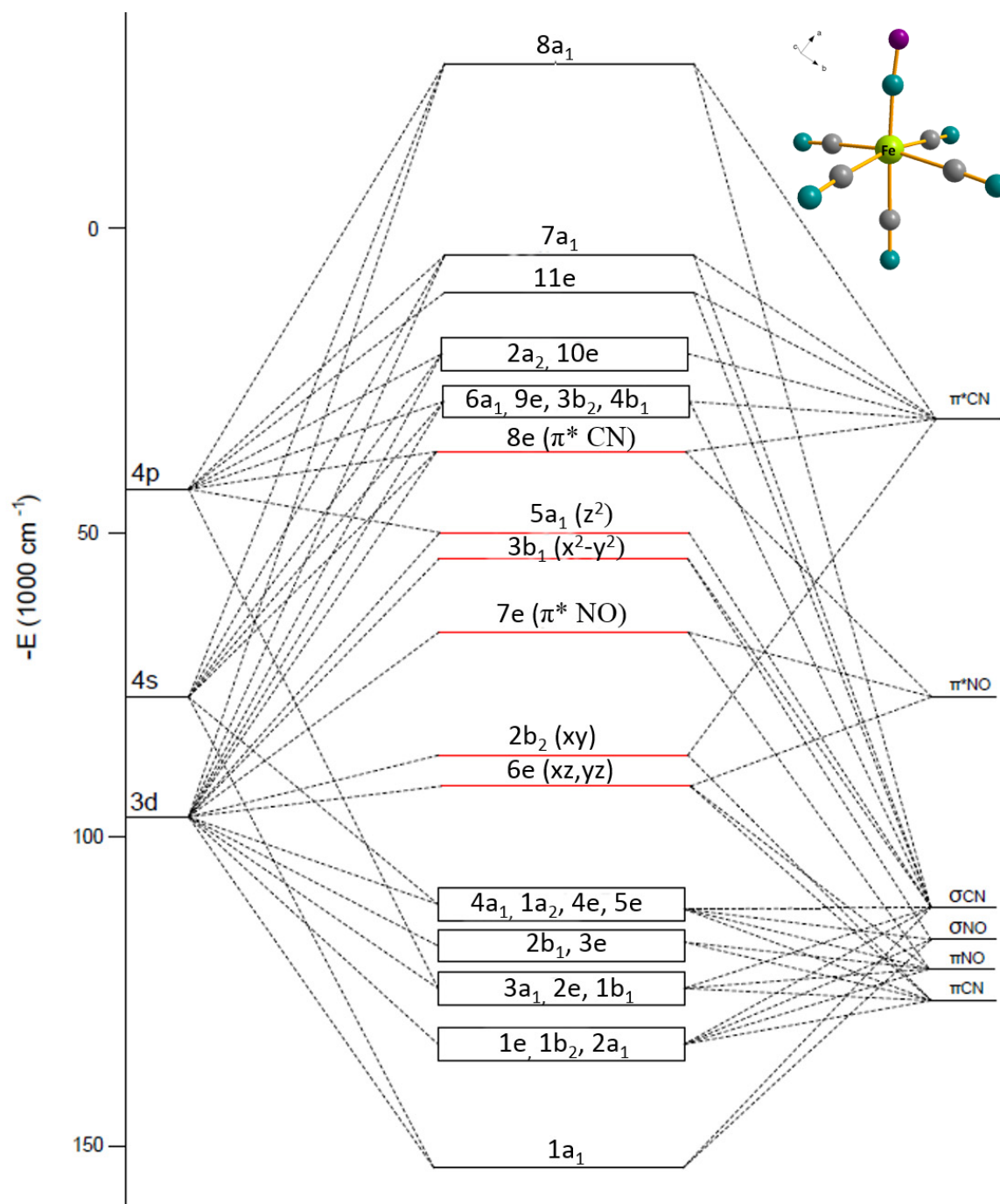


Figure S20: Molecular energy levels diagram for the nitroprusside ion, $[\text{Fe}(\text{CN})_5\text{NO}]^{2-}$, adapted from Reference 46